



# Computational modeling of ovarian cancer dynamics suggests optimal strategies for therapy and screening

Shengqing Gu<sup>a,b,1</sup>, Stephanie Lheureux<sup>a,c</sup>, Azin Sayad<sup>a</sup>, Paulina Cybulska<sup>a,d</sup>, Liat Hogen<sup>a,d</sup>, Iryna Vyarvelska<sup>a,d,2</sup>, Dongsheng Tu<sup>e</sup>, Wendy R. Parulekar<sup>e</sup>, Matthew Nankivell<sup>f</sup>, Sean Kehoe<sup>g</sup>, Dennis S. Chi<sup>h,i</sup>, Douglas A. Levine<sup>j</sup>, Marcus Q. Bernardini<sup>a,d</sup>, Barry Rosen<sup>a,d,3</sup>, Amit Oza<sup>a,c</sup>, Myles Brown<sup>k,l,4</sup>, and Benjamin G. Neel<sup>a,b,4,5</sup>

<sup>a</sup>Princess Margaret Cancer Center, University Health Network, Toronto, ON M5G 2M9, Canada; <sup>b</sup>Department of Medical Biophysics, University of Toronto, Toronto, ON M5G 1L7, Canada; <sup>c</sup>Division of Medical Oncology and Hematology, University of Toronto, Toronto, ON M5G 2M9, Canada; <sup>d</sup>Division of Gynecologic Oncology, University of Toronto, Toronto, ON M5G 2M9, Canada; <sup>e</sup>Canadian Cancer Trials Group, Queens University, Kingston, ON K7L 3N6, Canada; <sup>f</sup>Medical Research Council Clinical Trials Unit, University College London, London WC1V6LJ, United Kingdom; <sup>g</sup>Institute of Cancer and Genomic Sciences, University of Birmingham, Birmingham B152TT, United Kingdom; <sup>h</sup>Gynecology Service, Department of Surgery, Memorial Sloan Kettering Cancer Center, New York, NY 10065; <sup>i</sup>Department of Obstetrics and Gynecology, Weill Cornell Medical College, New York, NY 10021; <sup>j</sup>Laura and Isaac Perlmutter Cancer Center, New York University–Langone Medical Center, New York, NY 10016; <sup>k</sup>Center for Functional Cancer Epigenetics, Dana-Farber Cancer Institute, Boston, MA 02215; and <sup>l</sup>Department of Medical Oncology, Dana-Farber Cancer Institute, Boston, MA 02215

Contributed by Myles Brown, May 7, 2021 (sent for review February 8, 2021; reviewed by Frances R. Balkwill and Olivier Gevaert)

**High-grade serous tubo-ovarian carcinoma (HGSC) is a major cause of cancer-related death. Treatment is not uniform, with some patients undergoing primary debulking surgery followed by chemotherapy (PDS) and others being treated directly with chemotherapy and only having surgery after three to four cycles (NACT). Which strategy is optimal remains controversial. We developed a mathematical framework that simulates hierarchical or stochastic models of tumor initiation and reproduces the clinical course of HGSC. After estimating parameter values, we infer that most patients harbor chemoresistant HGSC cells at diagnosis and that, if the tumor burden is not too large and complete debulking can be achieved, PDS is superior to NACT due to better depletion of resistant cells. We further predict that earlier diagnosis of primary HGSC, followed by complete debulking, could improve survival, but its benefit in relapsed patients is likely to be limited. These predictions are supported by primary clinical data from multiple cohorts. Our results have clear implications for these key issues in HGSC management.**

ovarian cancer | computational model | neoadjuvant chemotherapy | primary debulking surgery

Ovarian cancer is the eighth most common cancer and cancer death in women worldwide (1). High-grade serous tubo-ovarian cancer (HGSC) constitutes ~70% of all ovarian malignancies and has the worst prognosis (2). Current treatment of most patients with HGSC consists of cytoreductive surgery and combination chemotherapy with platinum-containing DNA–cross-linking drugs and taxane-based microtubule-stabilizing agents (2). Although treatment significantly improves survival, most women relapse with chemotherapy-refractory disease and eventually succumb (3). Multiple mechanisms of chemoresistance have been documented (4, 5), including reduced intracellular drug accumulation (6), detoxification by increased levels of glutathione (7), altered DNA damage repair (8, 9), dysfunctional apoptotic pathways (10, 11), and hyperactivation of various cell signaling pathways (12–14). These mechanistic studies are consistent with recent genomic analyses that reveal marked clonal evolution of HGSC during therapy (15). Other evidence, however, supports a hierarchical organization of HGSC, featuring intrinsically chemoresistant “cancer stem cells” (CSCs) that can escape initial treatment and seed recurrence (16–18).

Although there is uniform agreement that HGSC patients should receive surgery and chemotherapy, the optimal order and timing of these modalities remain controversial. Two main options exist: primary debulking surgery with adjuvant chemotherapy (PDS), or neoadjuvant chemotherapy, followed by interval debulking surgery (NACT) (19–24). In either case, the surgical standard of care is to seek maximal cytoreduction, with the objective being to leave no visible residual disease. However, the precise definition of such

“optimal debulking” can vary among different centers, surgeons, and reports (19, 21, 24, 25).

Several studies have found similar outcomes after PDS or NACT, including two highly influential randomized trials (EORTC and CHORUS) carried out across multiple countries (22, 23, 26–28). In both trials, however, the question of potential bias in patient recruitment has been raised, favoring potentially those with more extensive disease, who are less likely benefit from “upfront” surgery (23, 28). Consistent with this interpretation, overall survival in these trials was significantly shorter than that seen in other HGSC cohorts (19, 24, 29, 30). Closer examination of these reports reveals additional factors that might have influenced their conclusions. The EORTC study had inconsistencies in optimal

Author contributions: S.G. and B.G.N. designed the study; S.G. constructed the computational model and performed the analyses; S.L., P.C., L.H., I.V., M.N., S.K., D.S.C., D.A.L., M.Q.B., B.R., and A.O. provided clinical expertise and critical therapeutic insights; A.S. provided computational and statistical expertise and helpful discussions; L.H. and I.V. extracted raw clinical data from the UHN dataset; D.T. and W.R.P. extracted raw clinical data from the CCTG dataset; M.B. and B.G.N. supervised the research; and S.G. and B.G.N. wrote the manuscript.

Reviewers: F.R.B., Barts and The London School of Medicine and Dentistry; and O.G., Stanford University.

Competing interest statement: D.S.C. reports personal fees from Bovie Medical Co. (now Apyx Medical), Verthermia Inc., C Surgeries, and Biom’Up. He is also a former stockholder of Intuitive Surgical Inc. and TransEnterix Inc. D.A.L. has a consulting/advisory role for Tesaro/GSK, Merck, and receives research funding to institution from Merck, Tesaro, Clovis Oncology, Regeneron, Agenus, Takeda, Immunogen, VBL Therapeutics, Genentech, Celis, Ambyr, and Splash Pharmaceuticals. He also is a founder of Nirova BioSense Inc. M.B. is a consultant to and receives sponsored research support from Novartis. M.B. is a consultant to and serves on the scientific advisory boards of Kronos Bio, H3 Biomedicine, and GV20 Oncotherapy. B.G.N. is a co-founder, holds equity in, and received consulting fees from Navire Pharmaceuticals, Northern Biologics Inc., and Jengu Therapeutics Inc. He also is a member of the Scientific Advisory Board and receives consulting fees and equity from Avrinis Inc., is a member of the Scientific Advisory Board and has equity in Recursion Pharma, received consulting fees from MPM Capital, and was an expert witness for the Johnson and Johnson ovarian cancer talc litigation in US federal court. His spouse has or held equity in Amgen Inc., Regeneron, Moderna Inc., Gilead Sciences Inc., and Arvinis Inc. F.R.B. was on a scientific advisory board of the department in Toronto run by A.O. in 2018. F.R.B. and D.A.L. are co-authors on a 2019 Commentary article.

Published under the PNAS license.

<sup>1</sup>Present address: Department of Medical Oncology, Dana-Farber Cancer Institute, Boston, MA 02215.

<sup>2</sup>Present address: Department of Obstetrics and Gynecology, McMaster University, Hamilton, ON L8S 4L8, Canada.

<sup>3</sup>Present address: Department of Gynecologic Oncology, Beaumont Hospital, Royal Oak, MI 48073.

<sup>4</sup>To whom correspondence may be addressed. Email: myles\_brown@dfci.harvard.edu or benjamin.neel@nyulangone.org.

<sup>5</sup>Present address: Laura and Isaac Perlmutter Cancer Center, New York University–Langone Medical Center, New York, NY 10016.

This article contains supporting information online at <https://www.pnas.org/lookup/suppl/doi:10.1073/pnas.2026663118/-DCSupplemental>.

Published June 14, 2021.

## Significance

The optimal timing of surgery/chemotherapy and the benefits of earlier diagnosis of HGSC remain controversial. We developed a mathematical framework of tumor dynamics, populated the model with primary clinical data, and reliably recapitulated clinical observations. Our model predicts that 1) PDS is superior to NACT with relatively small tumor burden and when complete debulking is feasible, 2) timely adjuvant chemotherapy is critical for the outcome of PDS with <1-mm residual tumors, 3) earlier detection of relapse is unlikely beneficial with current therapies, and 4) earlier detection of primary HGSC could have substantial benefit. These results provide insights into the evolutionary dynamics of HGSC, argue for new clinical trials to optimize therapy, and are potentially applicable to other tumor types.

debulking rates between participating centers, with the PDS-associated complete debulking data highly influenced by the results from a single institution (23). The CHORUS study involved 76 clinical sites, and there were substantial differences in surgery execution and chemotherapy drug selection/dosage between them (28).

At Princess Margaret Cancer Center, retrospective data showed that PDS patients with no visible disease postresection survived substantially longer (7-y survival, >60%) than those receiving NACT (7-y survival, ~10%). Furthermore, although residual tumor postresection is a critical determinant of survival, its influence on the PDS group was far more dramatic than on NACT group (24). Of course, this report suffers from deficiencies common to all retrospective analyses, including lack of randomization to account for tumor burden at diagnosis and other factors; indeed, the NACT group in this study did have more extensive disease.

Another controversy in HGSC management focuses on the potential benefit of earlier diagnosis. Earlier diagnosis of primary HGSC is generally assumed to enhance patient survival and quality of life (3). Intuitively, one might predict that the same reasoning would apply to recurrent disease; however, survival is similar in relapsed patients treated earlier, based on increasing serum CA125 levels, than in those treated only when physical symptoms of recurrence appear (31). Conceivably, the lead time between CA125 rise and clinical recurrence is too short for earlier chemotherapy to be beneficial; if so, then patient survival might be extended by more sensitive methods, such as testing for circulating tumor DNA (ctDNA) (32, 33).

To address these issues, we developed a mathematical framework that models the dynamics of HGSC progression, response to surgery and chemotherapy, and recurrence. Our results, generated over a wide range of parameters and accounting for hierarchical and stochastic models of tumor initiation, argue that PDS is superior to NACT when complete debulking is feasible and suggest that, with currently available therapies, the benefits of earlier detection are intrinsically restricted to primary HGSC.

## Results

**Clinical Cohorts.** To train and evaluate our model, we used two independent cohorts, comprising a total of 285 International Federation of Gynecology and Obstetrics (FIGO) stage IIIC–IV HGSC patients (Table 1 and *SI Appendix*, Fig. S1). The first dataset contains information on 148 patients who were treated by PDS or NACT at University Health Network (UHN) between March 2003 and November 2011 (24). In this cohort, “complete debulking” (no visible disease, operationally defined here as <1-mm residual tumor) was achieved in 97 patients, whereas 51 patients had 1–10 mm of residual tumor. Among the 97 patients with complete debulking, 40 received upfront surgery, followed by six cycles of platinum and taxane-based chemotherapy (hereafter,

“PDS <1 mm”), whereas the other 57 patients were treated with upfront chemotherapy, followed by interval surgery after the first three to four cycles (hereafter, “NACT <1 mm”). For each patient, descriptions of tumor size postsurgery and serum CA125 levels over the course of treatment were recorded (Fig. 1A). As reported previously (24), overall survival was much better for patients in the PDS <1-mm group (Fig. 1B). However, patients in the NACT <1-mm group tended to have greater tumor burden at diagnosis (24), confounding direct comparison of the survival curves. Data from these patients (termed “Training Set” below) were used to train the parameters in our computational model.

The other 51 patients in the UHN dataset underwent debulking but were left with residual tumor of 1–10 mm in diameter. Lack of complete gross debulking usually was due to tumor location. As reported previously (24), there was a significant negative association between residual tumor size and patient survival in patients who had undergone PDS (Fig. 1C), but no association was found in the NACT group (Fig. 1D). Similar trends have been observed in several other studies investigating the association between patient survival and residual tumor size (19, 20, 34). Independent of the <1-mm cohort, we used this 1- to 10-mm cohort (“Validation Set 1” below) in initial tests of the validity of our computational model (*SI Appendix*, Fig. S1).

The second dataset, which is independent of the UHN cohort, contains information on 137 patients diagnosed from October 2001 to June 2005 and enrolled in the CAN–Canadian Cancer Trials Group (CCTG)–OV16 trial (hereafter, “CCTG cohort”). These patients all received upfront surgery, followed by eight cycles of carboplatin/paclitaxel chemotherapy. The median delay for chemotherapy after surgery was 0.8 mo (compared with 1 mo at UHN). In 20 patients, debulking to <1-mm residual tumor was achieved, 36 patients had 1- to 10-mm residual tumor, and 81 patients had residual tumor diameter >10 mm. Data from the CCTG cohort were used to further evaluate the validity of our computational model (*SI Appendix*, Fig. S1).

**Model Overview.** We developed a mathematical model of cancer initiation and evolution to investigate the dynamics of HGSC growth, the onset of chemoresistance, and the effects of various treatment strategies on patient survival (Fig. 1E and detailed in *SI Appendix, Methods*). Our initial framework was based on work by the Michor laboratory (35, 36) and considers exponential expansion of HGSC cells starting from a single cancer cell that has all of the genetic alterations needed for proliferation and metastasis but has not developed chemoresistance. This framework assumes that during tumor development/progression, any chemosensitive HGSC cell can acquire mutations and/or epigenetic alterations that enable chemoresistance; i.e., it assumes a stochastic model of tumor initiation. However, the model can be modified to accommodate a hierarchical organization of HGSC, in which a relatively chemoresistant CSC gives rise to chemosensitive progeny. Importantly, the predictions/implications of the hierarchical and stochastic models are essentially the same (see *Materials and Methods* and *SI Appendix* for more details).

**Estimation of Parameter Values.** For most model parameters, a clinically relevant range of values could be deduced from clinical data or previous publications (see *Materials and Methods* for detailed description of parameter value estimations). We then varied  $u$  (the probability of conversion of a chemosensitive cell to a chemoresistant cell in each cell division) and  $\varepsilon$  (the proportion of cancer cells outside the peritoneum and unresectable) over a wide range and computed the expected distribution of survival of patients by Monte Carlo simulation. We compared the deviation between the Training Set data and the predictions of our model for each combination of  $u$  and  $\varepsilon$ , and from the region of best fit for these parameters, we inferred that  $10^{-9} < u < 10^{-7}$  and  $10^{-9} < \varepsilon < 10^{-5}$  (Fig. 2A). Finer investigation of the fit between data and

**Table 1. Patient characteristics in UHN and CTG cohorts**

		UHN cohort	CTG cohort
Total no. of patients		148	137
Time of diagnosis*		2008 Jan. (2005 Oct. to 2009 March)	2003 Nov. (2003 Jan. to 2004 Aug.)
Age*		58 (50–66)	58 (52–64)
Treatment regimen	PDS	61 (41%)	137 (100%)
	NACT	87 (59%)	0 (0%)
FIGO stage	IIIC	124 (84%)	102 (74%)
	IV	24 (16%)	35 (26%)
Residual disease	<1 mm	97 (66%)	20 (15%)
	1–10 mm	51 (34%)	34 (25%)
	>10 mm	0 (0%)	83 (60%)
CA125 before treatment*		686 (220–1,680)	Unknown
Overall survival*		41 (22: not reached)	40 (26: not reached)

\*Values indicate median (range of first and third quartiles).

theory in this parameter region showed that  $u = 10^{-7.6}$  and  $\varepsilon = 10^{-7.4}$  is the best combination of these parameters, as it minimizes the deviation between data and theory (Fig. 2B). Importantly, the trained value for  $u$  is consistent with chemoresistant conversion rates estimated for multiple other cancers (37–40). The trained value for  $\varepsilon$  predicts that inaccessible cancer cells outside the peritoneum are less numerous than cancer cells inside the peritoneum after first-line therapy, which comports with clinical observations that recurrent HGSC occurs predominantly inside the abdominal cavity. Using the trained parameter values, we compared the observed (Fig. 1B) and predicted (Fig. 2C) distributions of patient survival in the Training Set. Reassuringly, the model predictions closely recapitulated the clinical observations (Fig. 2D and E). Although this combination of  $u$  and  $\varepsilon$  yielded the best prediction using Training Set data, and big deviations from these values led to worse predictions (SI Appendix, Fig. S2 A and B), adjusting their values over a smaller range did not lead

to substantial decrease in prediction accuracy (SI Appendix, Fig. S2C). Therefore, in our follow-up analyses, in addition to using the base values of  $u = 10^{-7.6}$  and  $\varepsilon = 10^{-7.4}$ , we also tried alternative combinations to test the robustness of our model predictions.

Using our mathematical framework and these estimated rates, we then calculated the probability (as a function of tumor burden) that chemoresistant cells are present at diagnosis (SI Appendix, Fig. S3A). Consistent with clinical and theoretical studies of other malignancies (37–39, 41–45), our model predicted that at least some chemoresistant cells are always present at the start of therapy for HGSC. We varied the values for each model parameter over a large range to test their influence on the calculated number of resistant cells at diagnosis: Within the ranges tested, this number almost always exceeds  $10^3$  (SI Appendix, Fig. S3 B–G).

**Model Validation.** To assess the accuracy of our mathematical framework and the validity of the estimated parameter values,

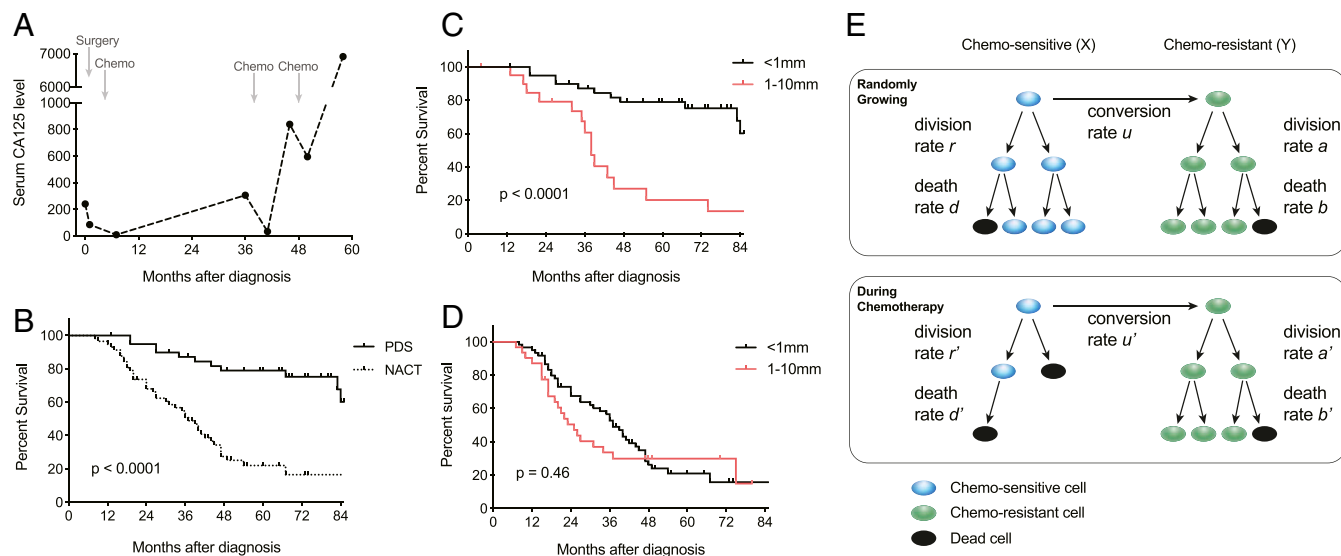


**Fig. 1. Mathematical framework of HGSC clinical course.** (A) Representative CA125 levels during clinical course of a typical HGSC patient. Chemotherapy responsiveness decreases along the treatment course, indicating the accumulation of chemoresistant cells. (B–D) Kaplan–Meier survival curves for patients in the UHN dataset. B compares the survival of patients with <1-mm residual tumor after treatment by PDS or NACT. Note that patients with PDS <1 mm lived significantly longer than those with NACT <1 mm ( $P < 0.0001$ ). C compares the survival of patients treated by PDS with <1-mm vs. 1- to 10-mm residual tumor. Note that patients with PDS <1 mm lived significantly longer than those with PDS 1–10 mm ( $P < 0.0001$ ). D compares the survival of patients treated by NACT with <1-mm vs. 1- to 10-mm residual tumor. Note that survival of these two groups was not significantly different ( $P = 0.46$ ). (E) Mathematical framework for modeling HGSC progression. The model assumes the existence of chemosensitive and chemoresistant HGSC cells. During random growth, chemosensitive cells divide at rate  $r$ , die at rate  $d$ , and convert into chemoresistant cells with probability  $u$  per cell division; chemoresistant cells divide at rate  $a$  and die at rate  $b$ . During chemotherapy, chemosensitive cells divide at rate  $r'$ , die at rate  $d'$ , and convert into chemoresistant cells with probability  $u'$  per cell division; chemoresistant cells divide at rate  $a'$  and die at rate  $b'$ . See text and SI Appendix, Methods for details.

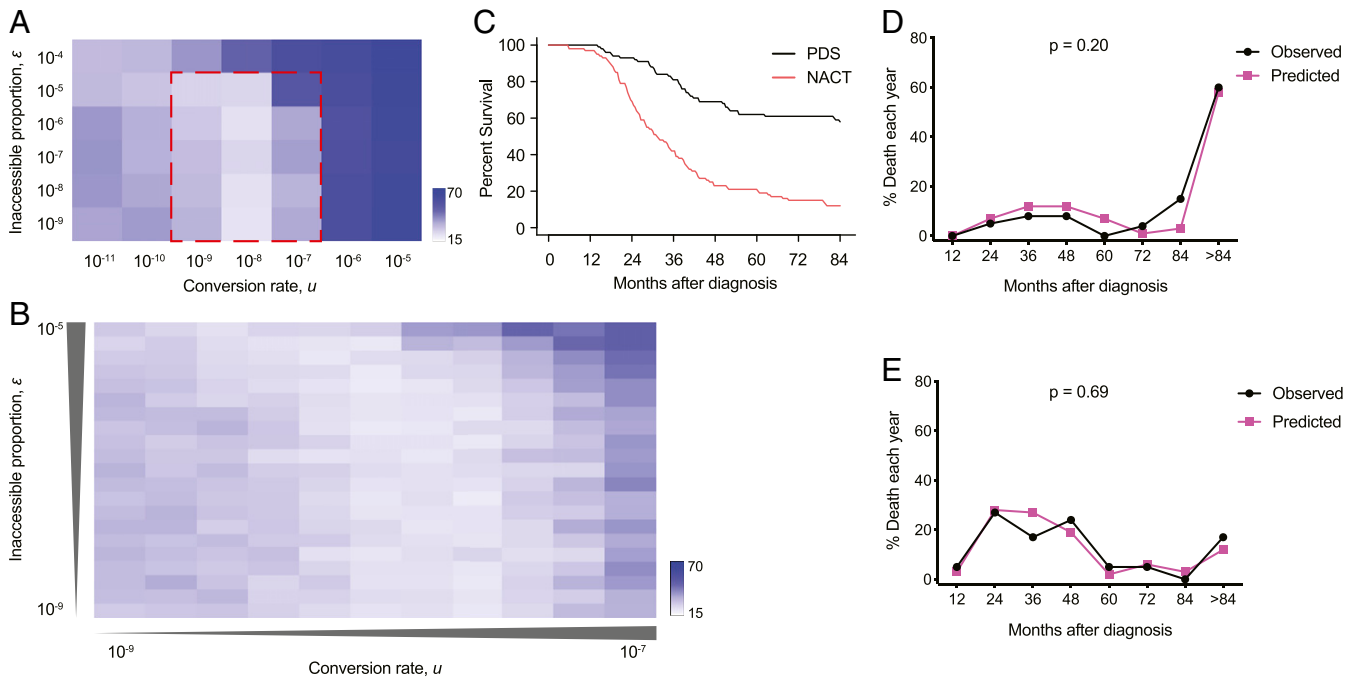


**Fig. 2.** Estimation of parameter values and evaluation of model predictions. (A and B) Estimation of conversion rate ( $u$ ) and inaccessible proportion ( $\epsilon$ ) in patients treated by PDS or NACT with  $<1$ -mm residual tumor, using data from the UHN cohort (Training Set). Colors represent the degree of deviation between clinical data and the predictions of the mathematical model. Lighter colors represent region of best fit between theory and observation. B provides a finer-scale analysis of the red dashed region in A. (C) Model prediction of survival of patients treated by PDS or NACT with  $<1$ -mm residual tumor. Parameter values are as follows:  $u = 10^{-7.6}$ ,  $\epsilon = 10^{-7.4}$ ,  $d = r/10$ ,  $b = a/10$ ,  $a' = a$ ,  $b' = a/5$ ,  $u' = 10u$ . Values for  $r$ ,  $a$ ,  $r'$ , and  $d'$  were obtained from normal distributions.  $r$  was set with mean of 2 and SD of 0.8.  $a$  was set with mean of 0.84 and SD of 0.42.  $r'$  was set with mean of 0.2 and SD of 0.08.  $d'$  was set with mean of 4.9 and SD of 1.  $M_1$ ,  $M_2$ , and  $M$  were obtained from normal distributions in the log-10 scale.  $\text{Log}_{10}M_1$  was set with mean of 11.5 and SD of 0.4 for PDS group and mean of 12 and SD of 0.4 for NACT group.  $\text{Log}_{10}M_2$  was set with mean of 13 and SD of 0.4.  $\text{Log}_{10}M$  was set with mean of 6 and SD of 0.4 for  $<1$ -mm residual cancer. (D and E) Comparisons of predicted and observed overall survival for PDS  $<1$ -mm (D) and NACT  $<1$ -mm (E) groups. There was no significant difference between the prediction and clinical data for D ( $P = 0.20$ ) or E ( $P = 0.69$ ).

we analyzed the model-predicted distribution of overall survival using data from several test sets (Fig. 3). First, we predicted the survival of patients in Validation Set 1 (Fig. 3A and B), by adjusting the value of  $M$  (the number of cancer cells left in the peritoneum after surgery), which can be approximated from the operative notes (categorized as “ $<1$  mm,” “ $1$ – $10$  mm,” or “ $>10$  mm”). Comparison of the observed (Fig. 3A) and predicted (Fig. 3B) distributions of patient survival revealed no significant differences (Fig. 3C and D).

The data for the above validation exercise were derived from different patients than those used for the Training Set, but both cohorts were treated over the same time period at the same institution (UHN). To more rigorously test the validity of our model, we analyzed independent patient data, derived from the CCTG cohort. As noted above, the treatment course of these patients also differed somewhat from that of the UHN patients, enabling an even better test of the general applicability of our framework. We incorporated these differences into the model and predicted the survival of patients in the CCTG trial. Again, the model predictions fit very well with clinical observations, and recapitulated the theme that PDS with minimal residual tumor results in the best outcome (Fig. 3E–I).

**Predicted Outcome of PDS and NACT in Patients with Identical Tumor Burden.** Confident in the predictive power of our mathematical framework, we modeled the expected clinical outcome of PDS and NACT in patients with the same initial tumor burden by imposing the same distribution of  $M_1$  on both groups. Our model predicts that PDS patients should survive longer than NACT patients when controlled for residual postsurgery tumor mass. As residual tumor increases, however, the predicted survival advantage of PDS shrinks (Fig. 4A and B). To investigate the underlying reason(s) for these

predictions, we explored the predicted dynamics of chemosensitive (blue) and chemoresistant (green) HGSC cells in patients undergoing treatment by PDS or NACT (Fig. 4C and D). Our model predicts that, at diagnosis, a typical HGSC patient has low numbers of chemoresistant cells. In women who undergo PDS, debulking surgery (S in Fig. 4C) dramatically reduces the number of chemosensitive and chemoresistant cancer cells, because these cells appear identical to the surgeon and therefore have an equal likelihood of removal. Depending on the (stochastic) distribution of chemoresistant cells within the abdominal cavity of the HGSC patient, all chemoresistant cells present at diagnosis might have been eliminated by complete debulking, with the residual chemoresistant cell number following a Poisson distribution. Follow-up chemotherapy (C in Fig. 4C) can then reduce the remaining chemosensitive cells to very low numbers or even eradicate them.

By contrast, with NACT, neo-adjuvant chemotherapy (C) dramatically enriches for chemoresistant cells while killing the sensitive cells; consequently, chemoresistant cells comprise a large proportion of total tumor cells at surgery (S). Because chemosensitive cells are largely depleted by the neoadjuvant chemotherapy, the amount of residual tumor visible to the surgeon is reduced substantially. Consequently, it is virtually impossible for interval debulking surgery to fully deplete the chemoresistant cells (Fig. 4D). We propose that this relative inability of NACT to deplete chemoresistant cells explains the difference in outcome from patients treated with PDS. Importantly, this conclusion is based on intrinsic properties of the dynamics of cancer proliferation, survival, and death.

We then explored why the predicted superiority of PDS over NACT depends on residual tumor burden postsurgery. By examining the expected distribution of chemosensitive and chemoresistant cell numbers after first-line therapy, we found that PDS with  $<1$ -mm

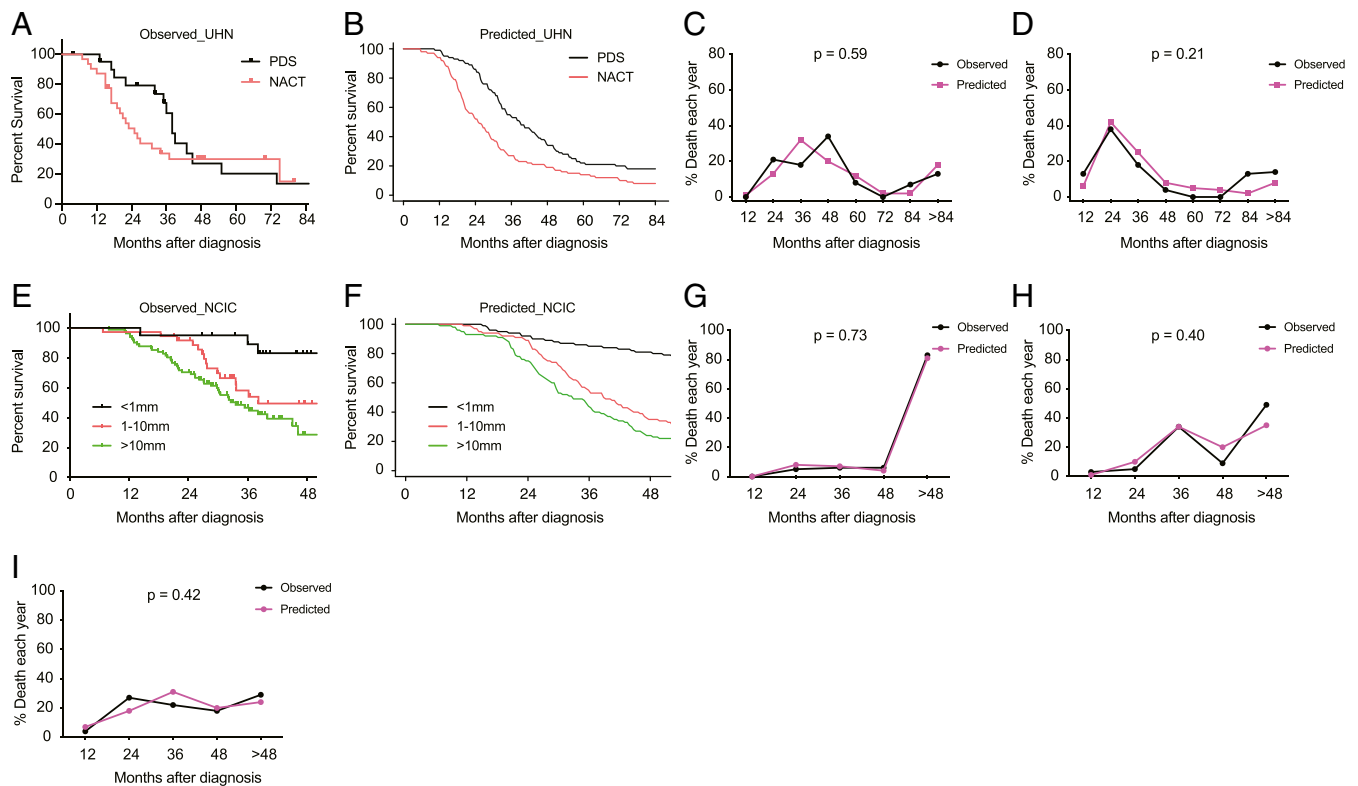


**Fig. 3.** Evaluation of model predictions with data from validation sets. (A and B) Observed (A) and predicted (B) overall survival of patients from the UHN dataset treated with PDS or NACT with 1- to 10-mm residual tumor. (C and D) Comparison of predicted and observed survival for the PDS (C) and NACT (D) 1- to 10-mm residual tumor groups. There was no significant difference between the predictions and clinical data for either (C) ( $P = 0.59$ ) or (D) ( $P = 0.21$ ). (E and F) Observed (E) and predicted (F) overall survival of patients in the CCTG cohort. Patients received PDS and had <1-mm, 1- to 10-mm, or >10-mm residual tumor. (G–I) Predicted and observed survival of PDS-treated patients from the CCTG study with <1-mm (G), 1- to 10-mm (H), or >10-mm (I) residual tumor. There was no significant difference between predictions and clinical data for G ( $P = 0.73$ ), H ( $P = 0.40$ ), or I ( $P = 0.42$ ). Parameter values were the same as in Fig. 2C, except that  $\log_{10}M$  was set with mean of 8 and SD of 0.4 for the 1- to 10-mm residual group, and mean of 10 and SD of 0.4 for the >10-mm residual groups. Also, the gap between surgery and the start of chemotherapy was 1 mo for the UHN patients and 0.8 mo for the CCTG patients; UHN patients received six cycles of chemotherapy for first-line PDS treatment, whereas CCTG patients received eight cycles.

residual tumor potentially can deplete all cancer cells in a significant proportion of HGSC patients (Fig. 4E). This finding can account for the considerable survival difference between PDS and NACT with <1-mm residual tumor. By contrast, with >1-mm residual tumor, neither PDS nor NACT depletes all malignant cells, even though fewer tumor cells are predicted to remain after PDS (Fig. 4F). Consequently, almost all patients with >1-mm residual tumor are predicted to relapse and eventually die because of the inability of current agents to kill chemoresistant cells. This analysis explains why PDS can be superior to NACT when complete debulking is achieved and why residual tumor mass is a key determinant of survival after PDS but not NACT (Fig. 3 A and B). Our predictions regarding PDS vs. NACT are illustrated in Fig. 4G.

**Test the Robustness and Generalizability of Model Prediction.** To test the robustness of our predictions and quantitatively examine the influence of each factor on survival, we varied each parameter in our model over a large range. We identified multiple factors that influence the magnitude of the predicted difference between PDS and NACT (SI Appendix, Fig. S4). For example, faster growth of cancer cells does not necessarily imply worse survival. Specifically, although elevated growth rate of chemoresistant cells in the absence of chemotherapy leads to worse survival, faster-growing, chemosensitive cells can sometimes result in better survival (SI Appendix, Fig. S4 A–D). This result can be attributed to a lower percentage of chemoresistant cells at diagnosis when chemosensitive cells proliferate faster. However, if the proliferation rate

of chemosensitive cells is too high (e.g., when  $r = 3$ ), new chemoresistant cells might be generated between the time of surgery and adjuvant chemotherapy, resulting in worse survival (SI Appendix, Fig. S4A). We also inferred that the relative importance of chemosensitive and chemoresistant cells in influencing survival might differ at different stages along the clinical course. During treatment-free periods, the growth rate of chemoresistant cells could play a more dominant role in influencing patient survival (SI Appendix, Fig. S4 A–D), because they underlie ultimate treatment failure. However, during periods of chemotherapy, the growth rate (or depletion rate) of chemosensitive cells might play a more dominant role (SI Appendix, Fig. S4 E–H), because the depletion rate of chemosensitive cells at this stage determines whether they can be completely eradicated by chemotherapy. By contrast, chemoresistant cells likely will endure. As a result, drug choice and dose, which likely influences the efficiency of elimination of chemosensitive cells, is predicted to be a critical factor in treatment outcome. Some molecular subgroups of HGSC (e.g., *CCNE1*-amplified tumors) are highly resistant to current chemotherapy. Our model predicts that these patients would be refractory to PDS, even if complete debulking is achieved (SI Appendix, Fig. S4 E and F, when  $r'$  is high or  $d'$  is low). Residual cancer cell abundance after tumor resection can dramatically influence patient survival, especially in the PDS group (SI Appendix, Fig. S4F), suggesting that primary cytoreductive surgery should aim for complete removal of cancer cells even though chemotherapy will usually follow. Tumor size at diagnosis can be a critical factor

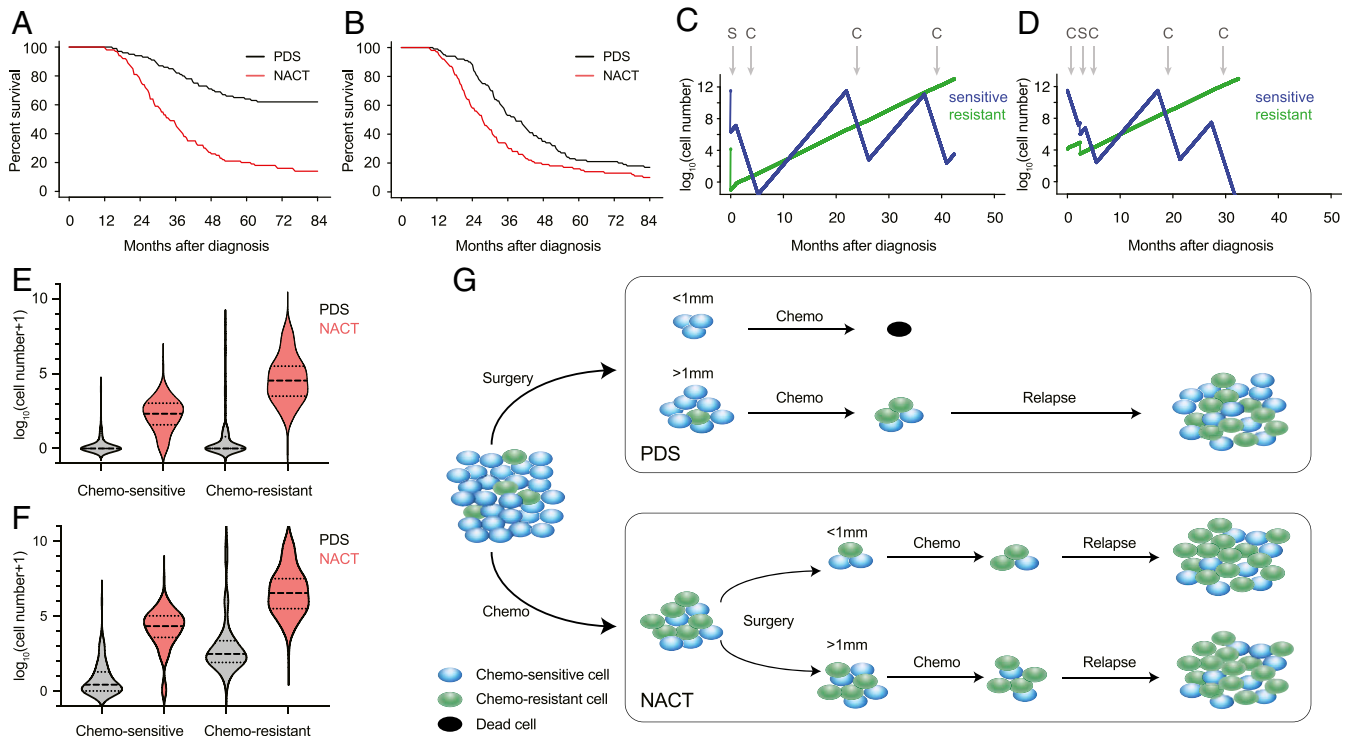


**Fig. 4.** Predicted outcome of PDS and NACT patients with same initial tumor burden. (A and B) Predicted survival of patients undergoing PDS (black curves) or NACT (red curves). All patients received six cycles of chemotherapy. A shows the results for <1-mm residual tumor group, and B shows the result for 1- to 10-mm residual tumor group. Parameter values were as in Fig. 2C, except that  $\log_{10}M_1$  was set at the same value for the PDS and NACT groups, with mean of 11.5 and SD of 0.4. (C and D) Simulation of representative progression dynamics for chemosensitive (green curves) and chemoresistant (blue curves) cancer cells in a patient undergoing PDS (C) or NACT (D) treatment with optimal debulking. Treatment order is shown at the top of each plot; “S” indicates “surgery,” and “C” indicates “chemotherapy.” (E and F) Distribution of number of chemosensitive and chemoresistant cells for the PDS (black curves) and NACT (red curves) groups, with <1-mm (E) or 1- to 10-mm (F) residual tumor. (G) Scheme illustrating HGSC clinical course following PDS or NACT treatment.

determining whether a patient can be cured (SI Appendix, Fig. S4J) and is addressed below. By contrast, varying the parameter value of tumor size at patient death did not influence the length of survival (SI Appendix, Fig. S4K).

To further test the general applicability of our model, we asked whether it could explain the similar outcome of patients treated with PDS and NACT in prospective clinical studies, such as the CHORUS trial (28), using their patient data. Overall, patients in this study had substantially shorter survival than cohorts in most other studies. We reasoned that this might be attributable to more severe disease at diagnosis in patients in this cohort, such as higher tumor burden and/or more severe systemic metastasis. We therefore retrained the parameters  $M_1$  and  $\epsilon$  for patients in the CHORUS study, only using the data from PDS or NACT 1- to 10-mm groups in this cohort. Indeed, the model predicted higher values for both parameters (median of  $M_1 = 10^{12.2}$  and  $\epsilon = 10^{-2.9}$ ) (SI Appendix, Fig. S5A). When we then use these parameter values to predict the survival of PDS and NACT <1-mm groups, the model predicted no significant difference between the two regimens, consistent with the trend published in the original study (28) (SI Appendix, Fig. S5B). These results indicate that the contradiction between existing retrospective studies and prospective trials might have derived from differences in disease severity at diagnosis of patients in each cohort. This analysis further supports the conclusion that disease burden information is a critical factor in choosing PDS or NACT. Importantly, our prediction is corroborated by a recent pooled analysis of the CHORUS and EORTC trials, which showed that PDS tends to outperform NACT in patients with stage IIIC but not stage IV disease (46).

We also considered two alternative scenarios: 1) that heterogeneous populations of (variably) chemoresistant cells exist in

the same patient (SI Appendix, Fig. S6 A–C), or 2) that HGSC initiates from an intrinsically chemoresistant “cancer stem cell,” which differentiates into chemosensitive “tumor progenitor cells” (SI Appendix, Fig. S6 D–F). Either of these assumptions results in the same conclusions as the original model.

**Modeling Alternative Treatment Regimens.** We next utilized our model to predict the effects of altering current treatment regimens on patient outcomes. For both PDS and NACT, adjuvant chemotherapy typically begins 4–5 wk postsurgery, an interval chosen to allow patients to recover from their typically aggressive surgical treatment. The length of the postsurgical chemotherapy delay varies between centers and among physicians, but its influence on treatment outcome has not been studied carefully. We varied the length of treatment delay in our model and tested the predicted effects on patient survival. For PDS with <1-mm residual tumor, earlier initiation of chemotherapy might prolong survival, whereas longer treatment delay might worsen outcome (Fig. 5A,  $P < 0.0001$ ). For PDS with >1-mm residual tumor or for NACT with any amount of residual tumor, treatment delay (within the same range) is predicted to have little effect on outcome (Fig. 5B–D). These differences arise primarily because upfront surgery that results in <1-mm residual tumor, followed by chemotherapy, potentially can deplete all tumor cells when treatment delay is minimized (Fig. 5E). The probability of depletion decreases with longer delay, largely because chemoresistant cells can arise during the gap between upfront surgery and adjuvant chemotherapy (Fig. 5E). By contrast, PDS with >1-mm residual tumor or NACT is unlikely to deplete all cancer cells (SI Appendix, Fig. S7 A–C), irrespective of treatment delay. Our predictions on the critical

nature of the interval between optimal debulking surgery and adjuvant chemotherapy are schematized in Fig. 5F.

Our model predicts that neoadjuvant chemotherapy enriches for chemoresistant cells and thus increases the percentage of chemoresistant tumor cells remaining postsurgery in patients treated with NACT. Conceivably, reducing the number of cycles of neoadjuvant chemotherapy might attenuate the enrichment for chemoresistant cells, and if the same number of residual cancer cells remain after surgery, less neoadjuvant chemotherapy might prolong survival. Indeed, our model predicts that patients undergoing NACT with <1-mm or >1-mm residual tumor could benefit slightly from reducing the number of presurgery chemotherapy cycles (SI Appendix, Fig. S7 D and E). The small predicted improvement arises primarily because of more efficient reduction of the number of chemoresistant cells at surgery. The benefit is limited, however, because for most patients, chemoresistant cells are still unlikely to be eradicated after their enrichment during the neoadjuvant chemotherapy period (SI Appendix, Fig. S7 F and G).

**Predicted Effects of Earlier Diagnosis on Survival.** We also utilized our model to evaluate the potential benefits of earlier diagnosis. We first modeled the effects of diagnosing relapsed HGSC at the earliest possible time enabled by the currently used clinical test, CA125 detection (47). Contrary to the intuitive notion that earlier diagnosis of recurrence should be advantageous, we find that CA125-based earlier diagnosis is not expected to improve survival (Fig. 6 A and B, red curves). We also asked whether detecting recurrence earlier than is possible with CA125 monitoring would be advantageous. However, even with a sensitivity  $\sim 10^4$  greater than that required for physical symptoms to appear (lead time, >5 mo), the current upper limit of sensitivity for ctDNA-based diagnosis of ovarian cancer (33), our model predicts no advantage in patient survival if recurrence is detected earlier (Fig. 6 A and B, green curves).

We explored the reason for this lack of survival advantage by modeling the theoretical numbers of chemosensitive and chemoresistant cells in a virtual patient whose recurrence is diagnosed with increasing levels of sensitivity (Fig. 6C). Although earlier diagnosis, followed by prompt reinstitution of chemotherapy, can better deplete chemosensitive cells, it barely affects the chemoresistant cells that have been enriched by first-line therapy, which ultimately expand and cause patient death. Therefore, earlier

diagnosis is unlikely to improve survival when applied to relapsed cancers treated with standard cytotoxic chemotherapy regimens. Based on this result, we asked whether treating relapsed tumors using a hypothetical drug with similar efficacy but a distinct resistance mechanism from platinum/paclitaxel would potentiate the benefit of earlier diagnosis of relapsed HGSC. Indeed, our model predicts that earlier diagnosis of relapsed cancer can be beneficial, but only with alternative second-line therapy (Fig. 6 D and E). The magnitude of the advantage of earlier diagnosis of relapse primarily depends on the probability that earlier, but not later, intervention at relapse can be curative. Our predictions on the impact of earlier detection of relapsed tumor are illustrated in Fig. 6F.

Finally, we used our model to explore the potential benefit of earlier detection of treatment-naive tumors. As HGSC deposits usually get larger and/or more disseminated if left untreated, earlier upfront diagnosis would likely identify smaller, probably less disseminated, tumors, potentially increasing the chances of complete debulking. We therefore focused our comparison on the predicted effects in patients with <1-mm residual tumor. Our analysis argues that earlier diagnosis of treatment-naive cancer, with concomitant prompt intervention, can improve patient survival compared to regular diagnosis when controlled for residual cancer cell number postsurgery (SI Appendix, Fig. S8). For PDS with complete debulking, the predicted survival benefit can be dramatic, primarily because lower volume and less diffuse tumor at presentation can increase the likelihood of disease eradication (SI Appendix, Fig. S8 A, C, and E). By contrast, for NACT with complete debulking, the predicted benefit is rather limited, and the difference is detectable only if lead time is sufficient (SI Appendix, Fig. S8 B, D, and F). In that case, chemoresistant cells might not yet have arisen, and chemotherapy alone might be sufficient to eradicate disease.

**Discussion**

Mathematical modeling has demonstrated potential in the systematic and quantitative assessment of various treatments (44, 48, 49). If the outcomes of different strategies could be modeled accurately a priori, clinical trials could focus on therapeutic combinations that are most likely to succeed, and improvements in patient outcomes could be accelerated. The potential benefits of

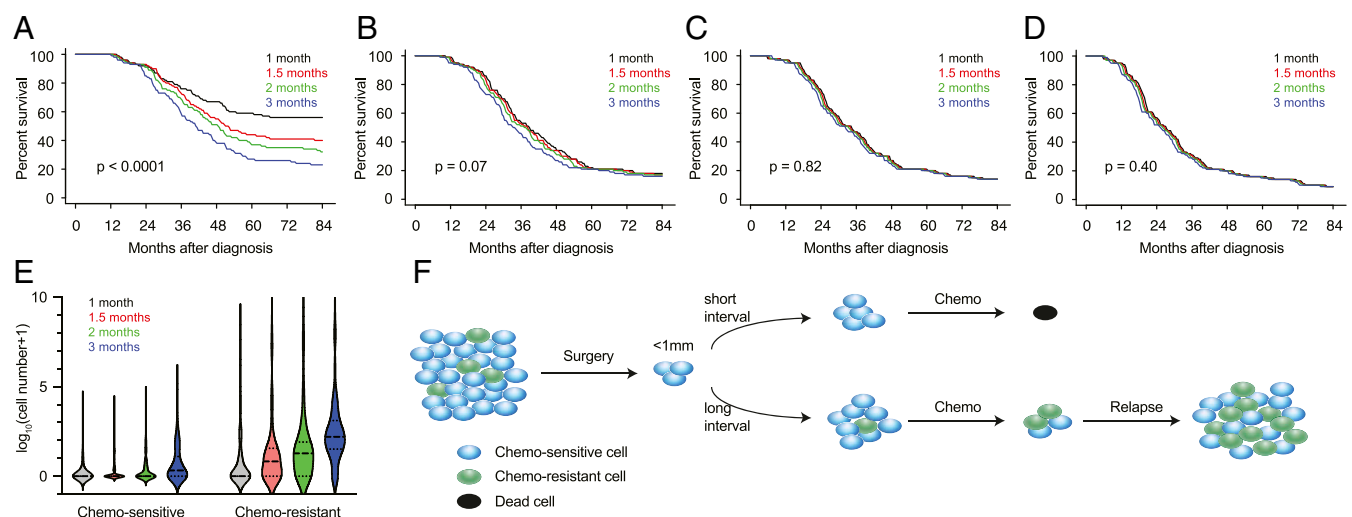


**Fig. 5.** Predicted outcomes of alternative treatment strategies. (A–D) Predicted survival of patients receiving PDS (A and B) or NACT (C and D) with different lengths of delay between debulking surgery and adjuvant chemotherapy. A and C show expected results with <1-mm residual tumor after surgery; B and D show predicted results with 1- to 10-mm residual tumor. (E) Distributions of the numbers of chemosensitive or chemoresistant cells after PDS (<1-mm residual tumor) with different intervals (colored lines) between debulking surgery and adjuvant chemotherapy. (F) Scheme showing predicted HGSC clinical course following PDS (<1-mm residual tumor) with standard or delayed adjuvant chemotherapy.

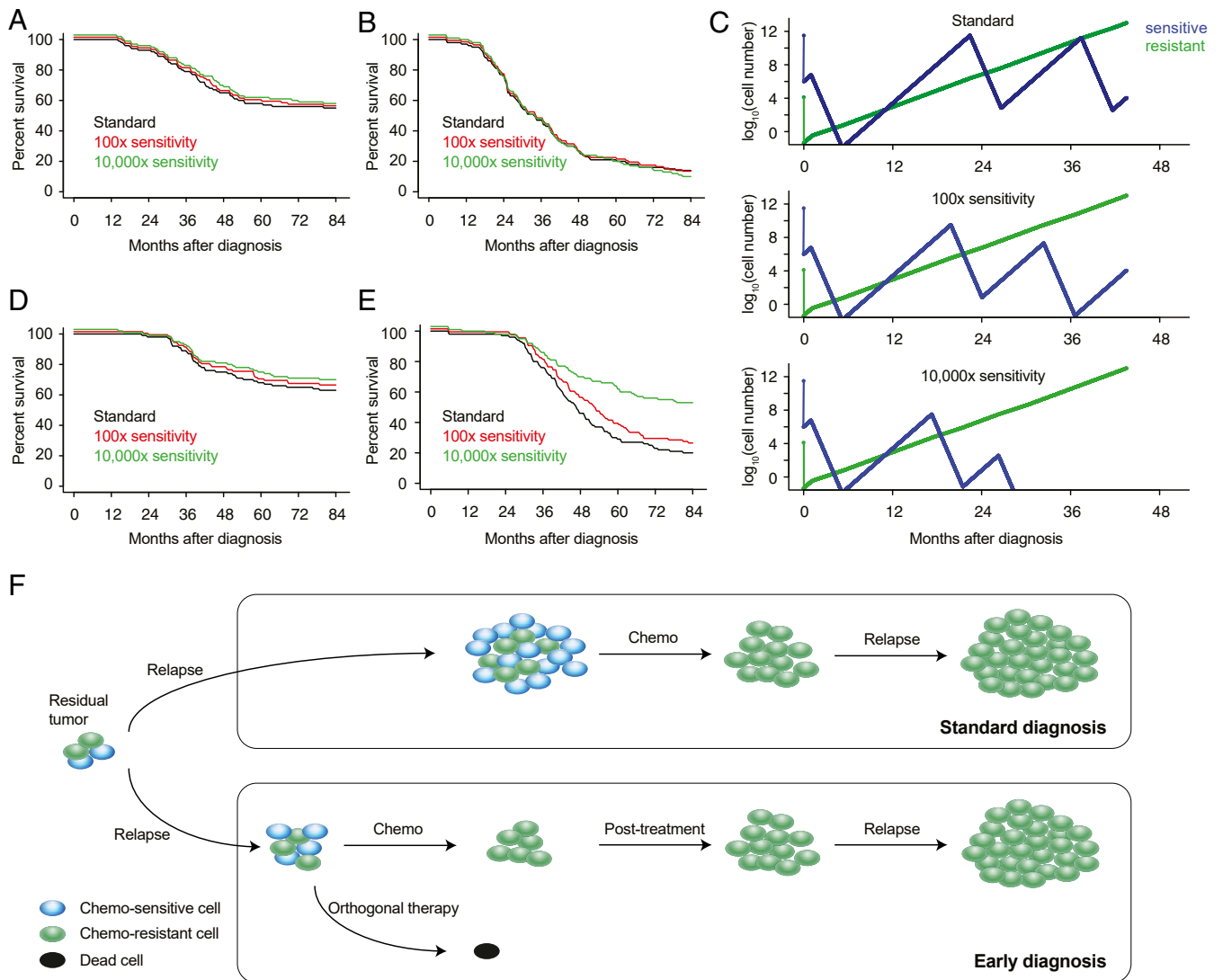


**Fig. 6.** Predicted effects of earlier diagnosis and treatment of relapsed cancer. (A and B) Predicted survival of patients with relapsed cancer detected at different degrees of sensitivity. Predictions were stratified based on the first-line therapy performed, including (A) PDS or (B) NACT with <1-mm residual tumor. “Standard” (black curves) represents diagnosis based on physical symptoms, when the number of cancer cells is comparable to  $M_1$ ; “100x sensitivity” (red curves) and “10,000x sensitivity” (green curves) represent earlier treatment of recurrent disease with the number of cancer cells at diagnosis 1% or 0.01% that of  $M_1$ , respectively. (C) Simulation of representative growth dynamics for chemosensitive (green curves) and chemoresistant (blue curves) cancer cells in a patient treated by PDS with optimal debulking, with relapsed cancer diagnosed at different degrees of sensitivity. Earlier treatment of relapsed cancer can more effectively deplete chemosensitive cells but does not effectively change the trajectory of chemoresistant cells, which are the ultimate cause of patient death. Parameter values are the same as in Fig. 2C. (D and E) Predicted survival of patients with relapsed cancer detected at different degrees of sensitivity and treated with a different second-line chemotherapy. Predictions were stratified based on the first-line therapy performed, including (D) PDS or (E) NACT with <1-mm residual tumor. “Standard” (black curves) represents diagnosis based on physical symptoms, when the number of cancer cells is comparable to  $M_1$ ; “100x sensitivity” (red curves) and “10,000x sensitivity” (green curves) represent earlier treatment of recurrent disease with the number of cancer cells at diagnosis 1% or 0.01% that of  $M_1$ , respectively. (F) Scheme showing predicted clinical course of relapsed HGSC, with standard or earlier diagnosis at relapse.

modeling are particularly important for diseases with relatively limited patient populations, in which it is not possible to do multiple clinical trials in parallel. Predictive models also can suggest when specific clinical controversies merit reexamination in the controlled trial setting. Our mathematical model of HGSC defines factors that affect the evolution of chemotherapy resistance and can predict patient survival based on the growth dynamics of chemosensitive and chemoresistant cells, whether stochastic or hierarchical models of tumor initiation are assumed. Our results have important implications for HGSC therapy and screening.

We populated our model with clinical data from ~300 patients receiving PDS or NACT. After estimating the rates of tumor cell proliferation and conversion to chemoresistance, we concluded that

most HGSC patients probably harbor chemoresistant cancer cells at diagnosis. Our outcome predictions closely match patient data from multiple sources and support clinical observations that 1) PDS that leaves minimal residual tumor is the optimal treatment strategy for patients who can tolerate the surgery and who do not have overwhelming or inaccessible disease burden at presentation; 2) residual tumor size is a critical determinant of survival in patients undergoing PDS, but not NACT; 3) earlier diagnosis of relapsed cancer does not—and cannot—lead to better survival with current therapies; and 4) earlier diagnosis of primary (treatment-naïve) HGSC could dramatically improve outcomes from this devastating disease, if PDS with complete debulking is feasible.



Our model shows clearly that, for HGSC patients whose tumor burden at diagnosis is not too severe, PDS with complete debulking should lead to a better outcome than NACT with complete debulking. We infer that the reason for the superior predicted outcome of PDS is that upfront surgery can deplete minority chemoresistant cells more effectively, leaving adjuvant chemotherapy to eradicate residual chemosensitive cells. If debulking surgery removes all chemoresistant cells, the PDS regimen can be curative. By contrast, cure is unlikely after NACT for at least two reasons. First, neoadjuvant chemotherapy enriches for, and allows the continued expansion of, chemoresistant cells. Second, by depleting bulk chemosensitive cells, chemotherapy removes tumor mass that can mark the location of chemoresistant cells interspersed in metastatic deposits. We suggest that removing these “sentinel” chemosensitive cells renders interval surgery less effective than upfront surgery in depleting chemoresistant cells, which are the cells that eventually cause death. At present, the most feasible way to achieve this goal is by surgically removing such cells, which is much more likely with the PDS regime. Of course, the development of drugs that can target these resistant cells should alter these conclusions (17, 22, 50).

Previous clinical studies differed over whether PDS or NACT is superior. A retrospective analysis of patients treated between 1980 and 1997 found no difference in outcome between PDS and NACT (26). By contrast, several meta-analyses indicated that NACT is associated with worse prognosis (21, 51). This controversy occasioned two large, controlled clinical trials to compare PDS and NACT (23, 28), which found no significant difference in patient survival between PDS and NACT. A major reason for these contradictions can be attributed to differences in study design and patient selection. Our model shows how these contradictions can be reconciled. For the retrospective studies, where patients underwent less preselection and thus are more likely to represent the bulk population, our model predicts that PDS should be superior to NACT with complete debulking. In the prospective studies, only patients with “extensive” HGSC were recruited, which might explain the notably worse outcome of patients in this study, especially in PDS <1-mm group, compared with multiple other reports (19, 20, 24, 52). Our computational model predicts that elevated upfront tumor burden should lead to worse overall survival and obscure the difference in outcome between PDS and NACT, even when complete debulking is performed (*SI Appendix, Figs. S4J and S5*). In particular, differences in the magnitude of  $\epsilon$ , the “inaccessible proportion,” alone might contribute to the lack of difference between PDS and NACT in these trials. This prediction is corroborated by a recent pooled analysis of the EORTC and CHORUS trials (46). Our results also imply that knowing the feasibility of complete debulking before surgery could assist in choosing PDS vs. NACT for treatment. Indeed, several studies reported that laparoscopy can be used for this purpose (53–55).

An earlier mathematical modeling study, based on a Gompertzian growth model, argued that NACT should be superior to PDS (56). However, that study did not account for the different dynamics of chemosensitive and chemoresistant cells and assumed equal efficiency of surgical depletion of large and small tumors, which ignores the intrinsic limitations of surgery. Such assumptions can lead to serious errors in modeling HGSC. For example, although aggressive surgery might reduce a tumor containing  $>10^{11}$  cells to a mass of  $<10^7$  cells, a tumor containing  $<10^6$  cells is unlikely to be visible during surgery, making it highly unlikely that such a tumor can be surgically reduced to  $<10^2$  cells.

A study of the optimal order of surgery and chemotherapy in pancreatic cancer concluded that neoadjuvant chemotherapy should be superior to upfront surgery (36). However, the biology and chemoresponsiveness of pancreatic cancer and HGSC differ substantially: Whereas HGSC is usually quite chemoresponsive, pancreatic cancer is notoriously chemoresistant. The differential influence on tumor visibility following chemotherapy likely underlies the different

predictions in the two diseases. Nevertheless, the difference between our conclusions and those of Haeno et al. (36) argue for caution in extrapolating their conclusions to other types of cancer.

Some treatment considerations are beyond the scope of computational modeling. For example, in many patients (e.g., the infirm), NACT is preferred simply because of the potential risks of this large operation, which include bowel perforation, uncontrolled bleeding, and/or the stresses of prolonged surgery/anesthesia. In such scenarios, treatment choice depends primarily on technical feasibility. Another limitation of our model is that we do not simulate potential effects of the tumor microenvironment (TME), including infiltrating immune cells. Recent studies from our group and by others suggest that the immune microenvironment of HGSC, shaped by tumor-initiating mutations, has a major influence on HGSC biology (57, 58). The paucity of data on immune landscape characterization in clinical samples and our limited understanding of the tumor-infiltrating immune cells at present preclude accurate simulation of such effects. With the increasing availability of clinical data and better mechanistic understanding of cancer-immune interaction, TME effects could be integrated into our model in the future.

Our model also enables quantitative analysis of the dependence of treatment outcome on various factors under different scenarios, providing a powerful tool to assist clinical decision-making. For example, we found that the advantage of PDS over NACT diminishes with larger residual tumor postsurgery, more extensive metastases at unresectable locations, and/or a higher percentage of chemoresistant cells at diagnosis (Fig. 3 *A* and *B* and *SI Appendix, Fig. S4A–C*). These features might help explain the similar overall survival between PDS and NACT groups in studies involving patients with more extensive upfront disease or less complete surgical removal (23, 26). Our analysis argues that for PDS patients with <1-mm residual tumor, adjuvant chemotherapy should start as early as possible to provide the best chance of curative outcome; indeed, we predict that differences of even a few weeks might dramatically alter the chance for curative outcome. Conversely, if complete debulking is not achieved at primary surgery, delaying chemotherapy is less likely to affect survival. These predictions are consistent with the results of a meta-analysis of clinical studies (59), which found that each extra week of delay was associated with a significantly decreased overall survival in patients with PDS <1-mm residual tumor, but not in patients with visible residual disease. We also predict that reducing the number of cycles of neoadjuvant chemotherapy might result in slightly improved overall survival for NACT patients, a prediction that is consistent with a meta-analysis (51) and a very recent clinical study (60). Recent work suggests that NACT alters the immune cells in the tumor to a more antitumor state and might prime the tumor to respond better to immunotherapy (61). Therefore, we speculate that fewer cycles of neoadjuvant chemo might enrich for chemoresistant cells to a more limited extent, while also activating the immune response.

A final prediction of our model is that earlier diagnosis should have quite different impact on relapsed vs. treatment-naïve patients. For the former, earlier diagnosis is unlikely to improve overall survival, primarily because earlier treatment of recurrent tumors with existing agents cannot deplete chemoresistant cells that have been enriched over the clinical course. This prediction matches very well with earlier clinical observations (31). Two scenarios might alter this conclusion: 1) if effective chemotherapy with a resistance profile orthogonal to platinum/taxane-based therapy were to become available at relapse; or 2) if effective debulking could be achieved at relapse. Effective drugs against HGSC remain a major clinical limitation (62, 63). PARP inhibitors, which are used as maintenance therapy following platinum-taxane therapy and especially effective in patients with homologous recombination deficiency (64), could serve as such alternative agents for relapsed cancer. If they have different resistance mechanisms from first-line therapy, our findings suggest employing such alternative agents as early as

possible upon tumor relapse. Furthermore, the use of such alternative agents at relapse can be beneficial compared with reusing the first-line drugs, even in the absence of earlier diagnosis (Fig. 6E vs. Fig. 6B). Similar proposals on combining drugs with orthogonal resistance profiles have been raised by others (37, 65). Surgery is not typically performed on recurrent HGSC, and its efficacy could be limited by the proportion of cancer cells at unresectable locations at disease relapse. Nevertheless, our model calls for reevaluation of feasibility and potential efficacy of secondary surgery for the benefit of earlier diagnosis. Consistent with our analysis, retrospective studies (66, 67) and a recent prospective trial (68) indicate that secondary surgery achieving complete debulking can be beneficial for HGSC patients with platinum-sensitive tumors.

By contrast, our model predicts that earlier diagnosis of treatment-naïve cancer could improve overall survival for at least two reasons: 1) Chemo-resistant cells are usually not enriched prior to treatment and earlier intervention can reduce the likelihood that significant numbers of these cells will arise; and 2) earlier upfront surgery has a better chance of removing all chemo-resistant cells, assuming that tumor cells have not diffused throughout the peritoneal cavity or seeded unresectable locations. This trend is consistent with a recent clinical trial testing the benefit of earlier upfront diagnosis of HGSC. Although screening did not identify ovarian cancer at an earlier stage, women who were screened annually for serum CA125 levels had reduced mortality from ovarian cancer than those with no screening (69). In that study, the survival improvement by CA125-based screening was significant but modest, and might be attributable to at least two factors: 1) the lead time of CA125-based screening is on average less than 1 y (70, 71), which is shorter than the screening interval; 2) early-diagnosed patients may receive either PDS or NACT, and our model predicts that particularly in this setting, NACT might counteract the benefit of earlier diagnosis. Two additional potential advantages of earlier diagnosis and treatment of naïve HGSC are not explicitly considered in this analysis: 1) Earlier diagnosis might increase the likelihood of complete debulking; and 2) patients considered treatable only by NACT with regular diagnosis might be eligible for PDS with earlier diagnosis.

In summary, our analyses suggest that future randomized clinical trials might consider 1) the influence of the interval between primary debulking surgery and adjuvant chemotherapy on treatment outcome, particularly for those with <1-mm residual disease, 2) the association between the number of neoadjuvant chemotherapy cycles and treatment outcome, 3) the effects of alternative chemotherapy and/or complete secondary surgery on relapsed tumor, especially when coupled to earlier diagnosis, and 4) better ways to estimate tumor mass at presentation, and thereby refine the prediction of which patients are most likely to benefit from PDS. Our results also argue that whereas not all patients who can achieve complete cytoreduction will benefit from PDS over NACT (give the importance of, and difficulty in measuring,  $\epsilon$ ), a subset of patients exist whose only chance of long-term survival or cure is the former regime. Finally, the mathematical abstraction makes our framework potentially applicable to evaluating different treatment strategies in other malignancies.

## Materials and Methods

**Patient Information.** Clinical data from 285 HGSC patients were obtained from patient records at UHN (148 patients) and from the CCTG OV16 NCT00028743 trial (137 patients). Medical record information, including date of diagnosis, age of patient, timing of treatment, extent of residual disease in diameter (<1, 1–10, or >10 mm), CA125 levels along the treatment course, and survival data (updated in 2014 for UHN data and 2010 for CCTG data) were recorded. Institutional research ethics board approval was obtained through UHN and a Data Sharing Agreement was concluded with CCTG.

**Variables Used in Mathematical Model.** We denote the following variables for the development of mathematical modeling:  $r$ , division rate of chemosensitive cells

in the absence of chemotherapy;  $d$ , death rate of chemosensitive cells in the absence of chemotherapy;  $a$ , division rate of chemo-resistant cells in the absence of chemotherapy;  $b$ , death rate of chemo-resistant cells in the absence of chemotherapy;  $r'$ , division rate of chemosensitive cells in the presence of chemotherapy;  $d'$ , death rate of chemosensitive cells in the presence of chemotherapy;  $a'$ , division rate of chemo-resistant cells in the presence of chemotherapy;  $b'$ , death rate of chemo-resistant cells in the presence of chemotherapy;  $M$ , the number of residual cancer cells in the peritoneal cavity after surgery;  $M_1$ , the total number of cancer cells at diagnosis;  $M_2$ , the total number of cancer cells at death;  $u$ , the probability of conversion of a chemosensitive cell to a chemo-resistant cell in each cell division;  $\epsilon$ , the proportion of cancer cells outside the peritoneum and unresectable.

**Estimation of Parameter Values.** Unless otherwise specified, clinically relevant parameter values were estimated and set as follows.

In the absence of chemotherapy, the proliferation rate of chemosensitive cells ( $r$ ) was obtained from the normal distribution with mean of 2 and SD of 0.8, based on a clinical study interrogating the doubling time of ovarian cancer cells by BrdU labeling (72). Another study compared cancer cell proliferation rates in platinum responders and nonresponders by thymidine labeling and found that responders had significantly higher labeling index than patients with stable or progressive disease (73). This analysis is consistent with several other studies that also found chemosensitive cells with proliferation advantage in the absence of therapy (74, 75). Accordingly, we set the proliferation rate of chemo-resistant cells ( $a$ ) to a normal distribution with mean of 0.84 and SD of 0.42. Death rates ( $d$  and  $b$ ) were set as 10% of proliferation rates ( $r$  and  $a$ ), respectively, which is within physiologically relevant range; in any case, varying this ratio over a large range does not affect the main conclusions of this paper.

During chemotherapy, the proliferation rate of chemosensitive cells ( $r'$ ) was set to 10% of that of randomly growing cells ( $r$ ); the death rate of chemosensitive cells ( $d'$ ) was set to a normal distribution with mean of 4.9 and SD of 1. These values were set to match the clinical observation that chemo-responsive relapse occurs on average ~11 mo after six cycles of chemotherapy, indicating that cytotoxic reduction of chemosensitive cells by six cycles of chemotherapy corresponds to ~11 mo of proliferation. Our inference is consistent with published efficacy of chemotherapy in HGSC (25, 76). The proliferation rate of chemo-resistant cells during chemotherapy ( $a'$ ) was set to the same as that during random growth ( $a$ ); the death rate of chemo-resistant cells during chemotherapy ( $b'$ ) was set to twice as that during randomly growing ( $b$ ), or 20% of  $a'$ , to reflect a modest effect of chemotherapy on chemo-resistant cells. Conversion rate during chemotherapy ( $u'$ ) was set as 10 times of that during randomly growing ( $u$ ), to reflect the DNA-damaging effect of platinum-based chemotherapy.

The parameters reflecting cancer cell numbers ( $M$ ,  $M_1$ ,  $M_2$ ) were obtained from normal distributions in base 10 logarithmic scale. The number of residual cancer cells immediately postsurgery ( $M$ ) was set to mean of 6 and SD of 0.4 on the log scale for <1-mm residual tumor, mean of 8 on the log scale for 1- to 10-mm residual cancer, and mean of 10 on the log scale for >10-mm residual cancer. The number of cancer cells at diagnosis ( $M_1$ ) was initially set at different values in patients receiving PDS and NACT, to reflect the clinical observation that patients with NACT tend to have more extensive disease at diagnosis (24).  $M_1$  for PDS was set at mean of 11.5 and SD of 0.4 on the log scale, and  $M_1$  for NACT was set at mean of 12 and SD of 0.4; these values result in NACT patients starting with >3× the cancer burden in the model than those receiving PDS. Moreover, we varied the ratio of tumor burden at diagnosis in NACT vs. PDS patients from 1 to  $10^{1.5}$ , and the main conclusions hold over the entire range.  $M_2$  was set to mean of 13 and SD of 0.4 on the log scale.

We varied the values for all of the above parameters to test the robustness of our conclusions. We found that the main conclusions hold true, although the magnitude of the differences between PDS and NACT treatment outcomes may vary.

**Mathematical Deduction of the Expected Number of Chemo-resistant Cells at Diagnosis.** We deduced the expected number of chemo-resistant cells at diagnosis based on previous studies (35, 36). We first calculated the probability that chemo-resistant cells exist at diagnosis ( $P_d$ ), and then calculated the expected number of chemo-resistant cells at diagnosis ( $Y_d$ ).

To calculate  $P_d$ , we summed the probabilities that the first successful lineage of chemo-resistant cells arises when there are 1, 2, 3, ...  $M_1-1$  chemosensitive cells.  $P(x)$  denotes the probability that the first lineage arises when there are  $x$  chemosensitive cells.  $P(x)$  can be expressed as the joint probability that no successful chemo-resistant lineage arises at 1, 2, 3, ...  $x-1$  chemosensitive cells, and that a successful lineage arises at exactly  $x$  chemosensitive cells. An expected  $1/(1-d/r)$  divisions are needed for an effective increase of 1 chemosensitive cell, and during these divisions an expected  $u/(1-d/r)$  chemo-resistant cells are

generated, among which a proportion  $(1 - b/a)$  will successfully persist. Assuming that the number of surviving chemoresistant cells generated by each division follows a Poisson distribution with mean  $(1 - b/a)u/(1 - d/r)$  (45), we derive  $P(x)$ :

$$P(x) = e^{-(x-1)(1-\frac{b}{a})u/(1-\frac{d}{r})} \left( 1 - e^{-(1-\frac{b}{a})u/(1-\frac{d}{r})} \right).$$

Thus, the probability that chemoresistant cells exist at diagnosis,  $P_d$ , can be written as the sum of  $P(x)$ :

$$P_d = \sum_{x=1}^{M_1-1} e^{-(x-1)(1-\frac{b}{a})u/(1-\frac{d}{r})} \left( 1 - e^{-(1-\frac{b}{a})u/(1-\frac{d}{r})} \right).$$

If we denote the time between the emergence of a successful chemoresistant cell and diagnosis as  $\tau_x$ , then the expected number of chemoresistant cells at diagnosis in the patients who have them can be expressed as follows:

$$Y_d = \frac{1}{P_d} \sum_{x=1}^{M_1-1} e^{-(x-1)(1-\frac{b}{a})u/(1-\frac{d}{r})} \left( 1 - e^{-(1-\frac{b}{a})u/(1-\frac{d}{r})} \right) e^{(a-b)\tau_x}.$$

The amount of time  $\tau_x$  satisfies the following:

$$xe^{(r-d)\tau_x} + e^{(a-b)\tau_x} = M_1.$$

**Simulation of the Dynamics of Cancer Cell Number after Diagnosis.** As the numbers of chemosensitive (denoted by  $X$ ) and chemoresistant (denoted by  $Y$ ) cells at diagnosis are expected to be large, we approximated their dynamics after diagnosis with a deterministic model, simulating the effects of random growth, chemotherapy, and surgery (cancer cell numbers before and after surgery are denoted as  $X_{before}$ ,  $Y_{before}$ , and  $X_{after}$ ,  $Y_{after}$  respectively):

$$\begin{aligned} \text{Random growth: } & \begin{cases} \frac{dX}{dt} = (r(1-u) - d)X \\ \frac{dY}{dt} = rY + (a-b)Y \end{cases}, \\ \text{Chemotherapy: } & \begin{cases} \frac{dX}{dt} = (r'(1-u') - d')X \\ \frac{dY}{dt} = r'Y + (a' - b')Y \end{cases}. \end{aligned}$$

1. F. Bray *et al.*, Global cancer statistics 2018: GLOBOCAN estimates of incidence and mortality worldwide for 36 cancers in 185 countries. *CA Cancer J. Clin.* **68**, 394–424 (2018).
2. B. T. Hennessy, R. L. Coleman, M. Markman, Ovarian cancer. *Lancet* **374**, 1371–1382 (2009).
3. G. C. Jayson, E. C. Kohn, H. C. Kitchener, J. A. Ledermann, Ovarian cancer. *Lancet* **384**, 1376–1388 (2014).
4. D. J. Stewart, Mechanisms of resistance to cisplatin and carboplatin. *Crit. Rev. Oncol. Hematol.* **63**, 12–31 (2007).
5. G. A. Orr, P. Verdier-Pinard, H. McDaid, S. B. Horwitz, Mechanisms of Taxol resistance related to microtubules. *Oncogene* **22**, 7280–7295 (2003).
6. S. C. Mann, P. A. Andrews, S. B. Howell, Short-term *cis*-diamminedichloroplatinum(II) accumulation in sensitive and resistant human ovarian carcinoma cells. *Cancer Chemother. Pharmacol.* **25**, 236–240 (1990).
7. P. Perego *et al.*, Ovarian cancer cisplatin-resistant cell lines: Multiple changes including collateral sensitivity to Taxol. *Ann. Oncol.* **9**, 423–430 (1998).
8. W. Zhen *et al.*, Increased gene-specific repair of cisplatin interstrand cross-links in cisplatin-resistant human ovarian cancer cell lines. *Mol. Cell. Biol.* **12**, 3689–3698 (1992).
9. X. Lin, S. B. Howell, Effect of loss of DNA mismatch repair on development of topotecan-, gemcitabine-, and paclitaxel-resistant variants after exposure to cisplatin. *Mol. Pharmacol.* **56**, 390–395 (1999).
10. P. J. Beale, P. Rogers, F. Boxall, S. Y. Sharp, L. R. Kelland, BCL-2 family protein expression and platinum drug resistance in ovarian carcinoma. *Br. J. Cancer* **82**, 436–440 (2000).
11. P. Perego *et al.*, Association between cisplatin resistance and mutation of p53 gene and reduced bax expression in ovarian carcinoma cell systems. *Cancer Res.* **56**, 556–562 (1996).
12. V. F. Chekhun, N. Y. Lukyanova, O. V. Urchenko, G. I. Kulik, The role of expression of the components of proteome in the formation of molecular profile of human ovarian

$$\text{Surgery: } \begin{cases} X_{after} = \frac{X_{before}}{X_{before} + Y_{before}} M + \varepsilon X_{before} \\ Y_{after} = \frac{Y_{before}}{X_{before} + Y_{before}} M + \varepsilon Y_{before} \end{cases}.$$

Treatment is adjudged a “failure” if the number of cancer cells posttreatment exceeds that pretreatment. In the case of treatment failure, our model simulates random growth of cancer cells to the total number of  $M_2$ , which marks patient death.

**Estimation of Conversion Rate  $u$  and Unresectable Proportion  $\varepsilon$ .** For each combination of candidate values for  $u$  and  $\varepsilon$ , we calculated the deviation of model prediction from clinical observations as follows:

$$Dev = \sqrt{\sum_i (\text{death}_{i-\text{th year observed}} - \text{death}_{i-\text{th year predicted}})^2}.$$

The combination that led to lowest deviation was used for model testing and further predictions.

**Statistical Analyses.** Comparisons of overall survival between two groups were performed by log-rank test. Comparisons of predicted survival between more than three groups were performed by log-rank test for trend when the order of groups is logical. Comparisons of distribution of overall survival between model predictions and clinical observations were performed by  $\chi^2$  test.

**Data Availability.** All study data are included in the article and/or supporting information.

**ACKNOWLEDGMENTS.** We thank Dr. Hiroshi Haeno from Kyushu University and Drs. Siv Sivalogathan and Mohammad Kohandel from Waterloo University for helpful discussions. This work was supported by grants from the Terry Fox Foundation (TFPG 020003), the National Cancer Institute (R37 49152 and R01257507), and the Mary Kay Foundation (to B.G.N.); and Doctoral Completion Award from University of Toronto and Sara Elizabeth O'Brien Trust Fellowship (to S.G.). D.S.C. is funded in part through the NIH/National Cancer Institute Cancer Center Support Grant P30 CA008748. B.G.N. was a Canadian Research Chair, Tier 1, and during that time, work in his laboratory was supported in part by a grant from the Ontario Ministry of Health and Long-Term Care and the Princess Margaret Cancer Foundation.

- carcinoma A2780 cells sensitive and resistant to cisplatin. *Exp. Oncol.* **27**, 191–195 (2005).
13. S. Lee, E.-J. Choi, C. Jin, D.-H. Kim, Activation of PI3K/Akt pathway by PTEN reduction and PIK3CA mRNA amplification contributes to cisplatin resistance in an ovarian cancer cell line. *Gynecol. Oncol.* **97**, 26–34 (2005).
14. B. Pan *et al.*, Reversal of cisplatin resistance in human ovarian cancer cell lines by a c-jun antisense oligodeoxynucleotide (ISIS 10582): Evidence for the role of transcription factor overexpression in determining resistant phenotype. *Biochem. Pharmacol.* **63**, 1699–1707 (2002).
15. A.-M. Patch *et al.*, Australian Ovarian Cancer Study Group, Whole-genome characterization of chemoresistant ovarian cancer. *Nature* **521**, 489–494 (2015).
16. J. M. Stewart *et al.*, Phenotypic heterogeneity and instability of human ovarian tumor-initiating cells. *Proc. Natl. Acad. Sci. U.S.A.* **108**, 6468–6473 (2011).
17. D. M. Janzen *et al.*, An apoptosis-enhancing drug overcomes platinum resistance in a tumour-initiating subpopulation of ovarian cancer. *Nat. Commun.* **6**, 7956 (2015).
18. B. Ffrench, C. Gasch, J. J. O'Leary, M. F. Gallagher, Developing ovarian cancer stem cell models: Laying the pipeline from discovery to clinical intervention. *Mol. Cancer* **13**, 262 (2014).
19. D. S. Chi *et al.*, An analysis of patients with bulky advanced stage ovarian, tubal, and peritoneal carcinoma treated with primary debulking surgery (PDS) during an identical time period as the randomized EORTC-NCIC trial of PDS vs neoadjuvant chemotherapy (NACT). *Gynecol. Oncol.* **124**, 10–14 (2012).
20. J. A. Rauh-Hain *et al.*, Primary debulking surgery versus neoadjuvant chemotherapy in stage IV ovarian cancer. *Ann. Surg. Oncol.* **19**, 959–965 (2012).
21. R. E. Bristow, E. L. Eisenhauer, A. Santillan, D. S. Chi, Delaying the primary surgical effort for advanced ovarian cancer: A systematic review of neoadjuvant chemotherapy and interval cytoreduction. *Gynecol. Oncol.* **104**, 480–490 (2007).
22. R. L. Coleman, B. J. Monk, A. K. Sood, T. J. Herzog, Latest research and treatment of advanced-stage epithelial ovarian cancer. *Nat. Rev. Clin. Oncol.* **10**, 211–224 (2013).

23. I. Vergote *et al.*, European Organization for Research and Treatment of Cancer-Gynaecological Cancer Group; NCIC Clinical Trials Group, Neoadjuvant chemotherapy or primary surgery in stage IIIC or IV ovarian cancer. *N. Engl. J. Med.* **363**, 943–953 (2010).
24. B. Rosen *et al.*, The impacts of neoadjuvant chemotherapy and of debulking surgery on survival from advanced ovarian cancer. *Gynecol. Oncol.* **134**, 462–467 (2014).
25. J. O. Schorge, C. McCann, M. G. Del Carmen, Surgical debulking of ovarian cancer: What difference does it make? *Rev. Obstet. Gynecol.* **3**, 111–117 (2010).
26. I. Vergote *et al.*, Neoadjuvant chemotherapy or primary debulking surgery in advanced ovarian carcinoma: A retrospective analysis of 285 patients. *Gynecol. Oncol.* **71**, 431–436 (1998).
27. A. Inciura *et al.*, Comparison of adjuvant and neoadjuvant chemotherapy in the management of advanced ovarian cancer: A retrospective study of 574 patients. *BMC Cancer* **6**, 153 (2006).
28. S. Kehoe *et al.*, Primary chemotherapy versus primary surgery for newly diagnosed advanced ovarian cancer (CHORUS): An open-label, randomised, controlled, non-inferiority trial. *Lancet* **386**, 249–257 (2015).
29. T. May *et al.*, The prognostic value of perioperative, pre-systemic therapy CA125 levels in patients with high-grade serous ovarian cancer. *Int. J. Gynaecol. Obstet.* **140**, 247–252 (2018).
30. V. D. Sioulas *et al.*, Optimal primary management of bulky stage IIIC ovarian, fallopian tube and peritoneal carcinoma: Are the only options complete gross resection at primary debulking surgery or neoadjuvant chemotherapy? *Gynecol. Oncol.* **145**, 15–20 (2017).
31. G. J. S. Rustin *et al.*; MRC OV05; EORTC 55955 investigators, Early versus delayed treatment of relapsed ovarian cancer (MRC OV05/EORTC 55955): A randomised trial. *Lancet* **376**, 1155–1163 (2010).
32. T. Forshew *et al.*, Noninvasive identification and monitoring of cancer mutations by targeted deep sequencing of plasma DNA. *Sci. Transl. Med.* **4**, 136ra68 (2012).
33. C. Bettgowda *et al.*, Detection of circulating tumor DNA in early- and late-stage human malignancies. *Sci. Transl. Med.* **6**, 224ra24 (2014).
34. A. Cervantes-Ruiperez *et al.*, Final results of OV16, a phase III randomized study of sequential cisplatin-topotecan and carboplatin-paclitaxel (CP) versus CP in first-line chemotherapy for advanced epithelial ovarian cancer (EOC): A GCG study of NCIC CTG, EORTC-GCG, and GEICO. *J. Clin. Oncol.* **31**, 5502 (2013).
35. H. Haeno, F. Michor, The evolution of tumor metastases during clonal expansion. *J. Theor. Biol.* **263**, 30–44 (2010).
36. H. Haeno *et al.*, Computational modeling of pancreatic cancer reveals kinetics of metastasis suggesting optimum treatment strategies. *Cell* **148**, 362–375 (2012).
37. I. Bozic *et al.*, Evolutionary dynamics of cancer in response to targeted combination therapy. *eLife* **2**, e00747 (2013).
38. I. Bozic, B. Allen, M. A. Nowak, Dynamics of targeted cancer therapy. *Trends Mol. Med.* **18**, 311–316 (2012).
39. L. A. Diaz Jr. *et al.*, The molecular evolution of acquired resistance to targeted EGFR blockade in colorectal cancers. *Nature* **486**, 537–540 (2012).
40. N. L. Komarova, D. Wodarz, Drug resistance in cancer: Principles of emergence and prevention. *Proc. Natl. Acad. Sci. U.S.A.* **102**, 9714–9719 (2005).
41. D. A. Landau *et al.*, Evolution and impact of subclonal mutations in chronic lymphocytic leukemia. *Cell* **152**, 714–726 (2013).
42. M. J. Ellis *et al.*, Whole-genome analysis informs breast cancer response to aromatase inhibition. *Nature* **486**, 353–360 (2012).
43. X. Ma *et al.*, Rise and fall of subclones from diagnosis to relapse in pediatric B-acute lymphoblastic leukaemia. *Nat. Commun.* **6**, 6604 (2015).
44. K. Leder *et al.*, Mathematical modeling of PDGF-driven glioblastoma reveals optimized radiation dosing schedules. *Cell* **156**, 603–616 (2014).
45. Y. Iwasa, M. A. Nowak, F. Michor, Evolution of resistance during clonal expansion. *Genetics* **172**, 2557–2566 (2006).
46. I. Vergote *et al.*; EORTC; MRC CHORUS Study Investigators, Neoadjuvant chemotherapy versus debulking surgery in advanced tubo-ovarian cancers: Pooled analysis of individual patient data from the EORTC 55971 and CHORUS trials. *Lancet Oncol.* **19**, 1680–1687 (2018).
47. M. J. Duffy *et al.*, CA125 in ovarian cancer: European group on tumor markers guidelines for clinical use. *Int. J. Gynecol. Cancer* **15**, 679–691 (2005).
48. J. Chmielecki *et al.*, Optimization of dosing for EGFR-mutant non-small cell lung cancer with evolutionary cancer modeling. *Sci. Transl. Med.* **3**, 90ra59 (2011).
49. L. G. de Pillis, A. E. Radunskaya, C. L. Wiseman, A validated mathematical model of cell-mediated immune response to tumor growth. *Cancer Res.* **65**, 7950–7958 (2005).
50. Y. Yu *et al.*, Inhibition of spleen tyrosine kinase potentiates paclitaxel-induced cytotoxicity in ovarian cancer cells by stabilizing microtubules. *Cancer Cell* **28**, 82–96 (2015).
51. R. E. Bristow, D. S. Chi, Platinum-based neoadjuvant chemotherapy and interval surgical cytoreduction for advanced ovarian cancer: A meta-analysis. *Gynecol. Oncol.* **103**, 1070–1076 (2006).
52. G. Hofstetter *et al.*, The time interval from surgery to start of chemotherapy significantly impacts prognosis in patients with advanced serous ovarian carcinoma—analysis of patient data in the prospective OVCAD study. *Gynecol. Oncol.* **131**, 15–20 (2013).
53. X. Deffieux, D. Castaigne, C. Pomel, Role of laparoscopy to evaluate candidates for complete cytoreduction in advanced stages of epithelial ovarian cancer. *Int. J. Gynecol. Cancer* **16**, 35–40 (2006).
54. A. Fagotti *et al.*, A laparoscopy-based score to predict surgical outcome in patients with advanced ovarian carcinoma: A pilot study. *Ann. Surg. Oncol.* **13**, 1156–1161 (2006).
55. N. R. Gómez-Hidalgo *et al.*, Predictors of optimal cytoreduction in patients with newly diagnosed advanced-stage epithelial ovarian cancer: Time to incorporate laparoscopic assessment into the standard of care. *Gynecol. Oncol.* **137**, 553–558 (2015).
56. M. Kohandel, S. Sivaloganathan, A. Oza, Mathematical modeling of ovarian cancer treatments: Sequencing of surgery and chemotherapy. *J. Theor. Biol.* **242**, 62–68 (2006).
57. S. Zhang *et al.*, Genetically defined, syngeneic organoid platform for developing combination therapies for ovarian cancer. *Cancer Discov.* **11**, 362–383 (2021).
58. S. Iyer *et al.*, Genetically defined syngeneic mouse models of ovarian cancer as tools for the discovery of combination immunotherapy. *Cancer Discov.* **11**, 384–407 (2021).
59. S. Mahner *et al.*, Prognostic impact of the time interval between surgery and chemotherapy in advanced ovarian cancer: Analysis of prospective randomised phase III trials. *Eur. J. Cancer* **49**, 142–149 (2013).
60. Y. L. Liu *et al.*, Pre-operative neoadjuvant chemotherapy cycles and survival in newly diagnosed ovarian cancer: What is the optimal number? A Memorial Sloan Kettering Cancer Center Team ovary study. *Int. J. Gynecol. Cancer* **30**, 1915–1921 (2020).
61. S. Böhm *et al.*, Neoadjuvant chemotherapy modulates the immune microenvironment in metastases of tubo-ovarian high-grade serous carcinoma. *Clin. Cancer Res.* **22**, 3025–3036 (2016).
62. C. Chester, O. Dorigo, J. S. Berek, H. Kohrt, Immunotherapeutic approaches to ovarian cancer treatment. *J. Immunother. Cancer* **3**, 7 (2015).
63. J. Lopez, S. Banerjee, S. B. Kaye, New developments in the treatment of ovarian cancer—future perspectives. *Ann. Oncol.* **24** (suppl. 10), x69–x76 (2013).
64. U. A. Matulonis, Management of newly diagnosed or recurrent ovarian cancer. *Clin. Adv. Hematol. Oncol.* **16**, 426–437 (2018).
65. E. Frei III, Combination cancer therapy: Presidential address. *Cancer Res.* **32**, 2593–2607 (1972).
66. P. Harter *et al.*; Arbeitsgemeinschaft Gynaekologische Onkologie Ovarian Committee; AGO Ovarian Cancer Study Group, Surgery in recurrent ovarian cancer: The Arbeitsgemeinschaft Gynaekologische Onkologie (AGO) DESKTOP OVAR trial. *Ann. Surg. Oncol.* **13**, 1702–1710 (2006).
67. S. M. Eisenkop, R. L. Friedman, N. M. Spirtos, The role of secondary cytoreductive surgery in the treatment of patients with recurrent epithelial ovarian carcinoma. *Cancer* **88**, 144–153 (2000).
68. A. Du Bois *et al.*, Randomized phase III study to evaluate the impact of secondary cytoreductive surgery in recurrent ovarian cancer: Final analysis of AGO DESKTOP III/ENGOT-ov20. *J. Clin. Oncol.* **38**, 6000 (2020).
69. I. J. Jacobs *et al.*, Ovarian cancer screening and mortality in the UK collaborative trial of ovarian cancer screening (UKCTOCS): A randomised controlled trial. *Lancet* **387**, 945–956 (2016).
70. G. L. Anderson *et al.*, Assessing lead time of selected ovarian cancer biomarkers: A nested case-control study. *J. Natl. Cancer Inst.* **102**, 26–38 (2010).
71. J. Bandyopadhyay, S. A. Ghamande, L. Zhang, L. Lan, M. S. Macfee, Lead time of rising CA-125 levels less than 35 u/ml predating radiologic confirmation of recurrent ovarian cancer. *J. Clin. Oncol.* **28**, e21072 (2010).
72. E. Erba *et al.*, Cell kinetics of human ovarian cancer with in vivo administration of bromodeoxyuridine. *Ann. Oncol.* **5**, 627–634 (1994).
73. A. Alama *et al.*, Tumour kinetics, response to chemotherapy and survival in primary ovarian cancer. *Eur. J. Cancer* **30A**, 449–452 (1994).
74. R. A. Gatenby, A. S. Silva, R. J. Gillies, B. R. Frieden, Adaptive therapy. *Cancer Res.* **69**, 4894–4903 (2009).
75. R. J. Gillies, D. Verduzco, R. A. Gatenby, Evolutionary dynamics of carcinogenesis and why targeted therapy does not work. *Nat. Rev. Cancer* **12**, 487–493 (2012).
76. A. L. Covens, A critique of surgical cytoreduction in advanced ovarian cancer. *Gynecol. Oncol.* **78**, 269–274 (2000).